



Published in final edited form as:

Acta Biomater. 2014 January ; 10(1): 40–46. doi:10.1016/j.actbio.2013.09.012.

Lysine-based polycation:heparin coacervate for controlled protein delivery

Noah Ray Johnson^{a,b}, Trisha Ambe^{c,d}, and Yadong Wang^{a,b,e,f,*}

^aDepartment of Bioengineering, University of Pittsburgh, Pittsburgh, PA 15219, USA

^bMcGowan Institute for Regenerative Medicine, Pittsburgh, PA 15219, USA

^cDepartment of Materials Science & Engineering, Carnegie Mellon University, Pittsburgh, PA 15219, USA

^dDepartment of Biomedical Engineering, Carnegie Mellon University, Pittsburgh, PA 15219, USA

^eDepartment of Chemical and Petroleum Engineering, University of Pittsburgh, Pittsburgh, PA 15219, USA

^fDepartment of Surgery, University of Pittsburgh, PA 15219, USA

Abstract

Polycations have good potential as carriers of proteins and genetic material. However, poor control over the release rate and safety issues currently limit their use as delivery vehicles. Here we introduce a new lysine-based polycation, poly(ethylene lysinylaspartate diglyceride) (PELD), which exhibits high cytocompatibility. PELD self-assembles with the biological polyanion heparin into a coacervate that incorporates proteins with high loading efficiency. Coacervates of varying surface charge were obtained by simple alteration of the PELD:heparin ratio and resulted in diverse release profiles of the model protein bovine serum albumin. Therefore, coacervate charge represents a direct means of control over release rate and duration. The PELD coacervate also rapidly adsorbed onto a porous polymeric scaffold, demonstrating potential use in tissue engineering applications. This coacervate represents a safe and tunable protein delivery system for biomedical applications.

Keywords

Polycation; Heparin; Lysine; Coacervate; Controlled release

1. Introduction

Polycations have good potential as carriers of proteins and genetic material. Chitosan and polyethylenimine (PEI) are two polycations commonly used in biomedical applications,

*Corresponding author. Address: 320 Benedum Hall, 3700 O'Hara St., Pittsburgh, PA 15261, USA. Tel.: +1 412 624 7196; fax: +1 412 524 3699., yaw20@pitt.edu (Y. Wang).

Disclosures

Scientific Protein Laboratories LLC donated the clinical-grade heparin. There are no patents, products in development or marketed products to declare. This does not alter our adherence to all Acta Biomaterialia policies on sharing data and materials.

including non-viral gene delivery [1–4], vaccine administration [5,6] and delivery of peptides [7,8]. However, safety risks associated with cytotoxicity and the accumulation of nanoparticles following delivery seriously limit their potential [9,10]. Poly(L-lysine) (PLL) has also been widely investigated as a delivery vehicle for proteins and DNA [11–14], though it has similar biocompatibility issues as PEI [15,16]. A synthetic polycation with good biocompatibility and controllable release rate would be highly beneficial for biomedical applications involving protein or gene therapy.

We have previously reported the synthesis of an arginine-based polycation, poly(ethylene argininy laspartate diglyceride) (PEAD), designed to complex with heparin to form a delivery matrix for heparin-binding growth factors [17]. PEAD:heparin self-assembles to form a coacervate, an assortment of organic molecules held together by polyvalent charge attraction and separated from the aqueous phase. We have demonstrated the use of this coacervate to deliver several factors for stimulating angiogenesis [18], accelerating cutaneous wound-healing [19] and improving heart function post-myocardial infarction [20,21]. In all cases the coacervate showed high loading efficiency, protection from degradation, sustained release over time and enhanced bioactivity compared to the growth factor in free-form. Having demonstrated that the coacervate satisfies the necessary functions of a delivery vehicle, we now address controllability of release rate by modification of the polycation and the coacervate composition.

The polyvalent and ionic nature of the coacervate makes modification of the charge density of the polycation one of the simplest ways to control release rate. Adjusting the polycation:heparin ratio in the coacervate is another simple way. The polycation and growth factor compete for ionic interaction with heparin; thus a coacervate with greater polycation content will compete more, resulting in faster growth factor release, while lower polycation content will slow release. Here we report a new polycation, poly(ethylene lysinyl aspartate diglyceride) (PELD), with lysine as the source of positive charge instead of arginine. PEAD has high biocompatibility [17], and here we demonstrate that the same design principle applies to lysine, thus PELD also has excellent biocompatibility. We describe the synthesis and characterization of PELD and its usefulness for controlled release.

2. Materials and methods

2.1. Materials

Ethylene glycol diglycidyl ether (EGDE) and trifluoroacetic acid (TFA) (TCI America, Portland, OR), t-BOC aspartic acid (BOC-Asp-OH) and t-BOC lysine (BOC-Lys) (Bachem, Torrance, CA), dimethylformamide (DMF), dichloromethane (DCM) and tetra-*n*-butylammonium bromide (TBAB) (Acros Organics, Geel, Belgium), dicyclohexylcarbodiimide (DCC) and *N*-hydroxysuccinimide (NHS) (Alfa Aesar, Ward Hill, MA), 4-dimethylaminopyridine (DMAP) (Avocado Research Chemicals, Lancaster, UK), polyethyleneimine (PEI; MW = 50–100 kDa) (MP Biomedicals, Santa Ana, CA), heparin sodium USP (MW = 16 kDa; Scientific Protein Labs, Waunakee, WI), fluorescein (Aldrich Chemical Co, Milwaukee, WI), bovine serum albumin (BSA) (Millipore, Billerica, MA) and poly(D,L-lactide-co-glycolide) 50:50 (PLGA) (Lakeshore Biomaterials, Birmingham, AL) were all used as received.

2.2. Synthesis of PELD

The intermediate, poly(ethylene aspartate diglyceride) (PED), was synthesized as previously described [17]. Briefly, EGDE (1.00 g) was combined with BOC-Asp-OH (1.34 g) and TBAB (5 mg) and dissolved in 0.6 ml of DMF. The mixture was maintained at 120 °C under N₂ for 20 min in a microwave synthesizer (Biotage, Uppsala, Sweden). DMF was evaporated under reduced pressure and TBAB was removed by multiple precipitations in diethyl ether. t-BOC was removed by stirring product in 4:1 DCM:TFA for 2 h. t-BOC lysine was conjugated to PED by DCC/NHS coupling. Briefly, BOC-Lys (0.692 g), NHS (0.323 g), DCC (0.753 g), and DMAP (5 mg) were dissolved in 5 ml DMF. PED (0.864 g) was dissolved in 5 ml of DMF in a separate vial. The two vials were then combined and stirred under N₂ for 24 h. An insoluble dicyclohexylurea by-product formed, and was removed by filtration at 0.22 µm. Finally, t-BOC was removed by stirring in pure TFA for 2 h and the product was purified by multiple precipitations in diethyl ether and then ethyl acetate.

2.3. Characterization of PELD

¹H nuclear magnetic resonance (NMR) spectroscopy was performed with a Biospin Avance NMR spectrometer (Bruker, Billerica, MA) using deuterium oxide (D₂O) solvent. The Fourier transformed infrared (FTIR) spectrum was recorded using a Nicolet IR-100 spectrometer (Thermo, Waltham, MA). Differential scanning calorimetry (DSC) was performed under nitrogen gas at a heating rate of 10 °C min⁻¹ using a Q200 differential scanning calorimeter (TA Instruments, New Castle, DE). The glass transition temperature (T_g) was determined using Universal Analysis 2000 software (TA Instruments) as the middle of the glass transition. Gel permeation chromatography (GPC) was performed on a Viscotek VE2001 system equipped with a 270 Dual Detector (differential refractive index and right angle light scattering) (Malvern Instruments, Westborough, MA). Two GRAM columns of 30 and 1000 Å porosities (PSS, Warwick, RI) and dimethylacetamide containing 3 g l⁻¹ lithium bromide and 6 ml l⁻¹ acetic acid were used as the stationary and mobile phases, respectively, and results were compared to polystyrene standards for calibration.

2.4. Preparation of polycation:heparin coacervates

PEAD, PELD and heparin were each dissolved in 0.9% saline and 0.22 µm filter-sterilized. The addition of either polycation to heparin immediately induced self-assembly of the coacervate, causing the complex to phase separate, visible as a turbid solution.

2.5. Zeta potential and dynamic light scattering (DLS) measurements

PELD and heparin were dissolved in deionized (DI) water at 10 and 1 mg ml⁻¹, respectively, then combined at PELD:heparin mass ratios of 2.5, 5, 7.5, 10, 12.5 and 15. Each coacervate solution was diluted to a 1 ml total volume with DI water. Zeta potential and particle size (hydrodynamic diameter) were both measured using a Zetasizer Nano ZS instrument (Malvern, Westborough, MA). From 10 to 20 readings were taken for each mass ratio and averaged.

2.6. Fluorescent imaging of PELD coacervates

PELD and heparin were dissolved in DI water at 10 mg ml^{-1} and fluorescein at $10 \text{ } \mu\text{g ml}^{-1}$. A $10 \text{ } \mu\text{l}$ volume of fluorescein was first mixed with heparin and then PELD was added to form coacervates with PELD:heparin mass ratios of 5, 10 and 15. The total mass of coacervate ($m_{\text{PELD}} + m_{\text{heparin}}$) was 1 mg for each, prepared in 0.1 ml of water. The coacervates were added to a 96-well plate and imaged immediately using a Nikon Eclipse Ti fluorescent microscope (Nikon Instruments, Melville, NY).

2.7. Cytotoxicity assay

PEAD was synthesized as previously described [17]. NIH 3T3 fibroblasts were seeded at 5×10^4 per well in a 96-well plate and cultured for 12 h at $37 \text{ }^\circ\text{C}/5\% \text{ CO}_2$ in Dulbecco's modified Eagle's medium containing 10% fetal bovine serum and 1% penicillin/streptomycin. The medium was then removed and culture medium containing PEAD, PELD or PEI at various concentrations (10, 1, 0.1, 0.01 mg ml^{-1}) was added to four wells per group. After 24 h, cells were washed once with Dulbecco's phosphate-buffered saline and the cell viability was assessed using a Live/Dead Assay (Molecular Probes, Eugene, OR) following the manufacturer's instructions. The results were normalized and compared to a control group which did not receive any polycation added to the media.

2.8. BSA release assay

PELD and heparin were each dissolved in 0.9% saline at 10 mg ml^{-1} . Heparin was initially combined with $500 \text{ } \mu\text{g}$ of BSA, then PELD was added to form mass ratios of 6, 8 and 10, corresponding to zeta potentials of approximately -10 , -5 and 0 mV , respectively. Tubes were stored at $37 \text{ }^\circ\text{C}$ under shaking conditions and, after 0, 1, 3, 7, 14 and 21 days, tubes were centrifuged at $12,000g$ for 5 min and the supernatant removed and frozen at $-20 \text{ }^\circ\text{C}$. After samples at all the time points had been collected, the BSA concentration was determined using the Pierce 660 nm Protein Assay (Thermo). In order to account for the protein content of the polycations and the heparin in the release fractions, results were normalized to an assay performed identically but without BSA.

2.9. Coacervate adsorption to polymer scaffolds

Porous PLGA scaffolds prepared by the salt-leaching technique were synthesized as previously described [22]. The scaffolds were 1 mm thick and 5 mm in diameter, with a 75–150 μm pore size. PELD and heparin were dissolved in deionized water at 5 mg ml^{-1} and combined at a 10:1 PELD:heparin mass ratio for maximal turbidity at charge neutrality. Next, 1.2 ml coacervate was added to a glass vial and stirred to prevent settling of the coacervate by gravity. A $50 \text{ } \mu\text{l}$ aliquot of coacervate was transferred to a cuvette and its optical density was read using a spectrophotometer (Biotek, Winooski, VT). PLGA scaffolds were then added to three separate vials and the coacervate was sampled and its optical density read in a similar fashion every 5 min. Three vials that did not receive any scaffold were used as controls. Digital images of the PELD coacervate-coated PLGA scaffold were taken at the endpoint, next to a bare PLGA scaffold.

2.10. Scanning electron microscopy

PELD and heparin were dissolved in deionized water at 10 mg ml^{-1} and combined at a 10:1 PELD:heparin mass ratio to form the coacervate. For coacervate imaging alone, $500 \mu\text{l}$ of coacervate was pipetted directly onto an aluminum stub. For PLGA scaffold coating, scaffolds were submerged in 1 ml of coacervate and soaked for 5 min, then mounted on aluminum stubs. Uncoated scaffolds from the same batch were also prepared. All samples were frozen and lyophilized overnight. Samples were sputter coated with gold to a 3.5 nm thickness and imaged using a JSM-633 OF scanning electron microscope (JEOL USA, Peabody, MA).

2.11. Statistical analysis

Statistical analysis was performed using SPSS 16.0 software (SPSS Inc, Chicago, IL). The data were tested for normality and equal variance before analysis. Statistical differences were calculated using one-way analysis of variance followed by Tukey's post hoc testing.

3. Results and discussion

3.1. PELD synthesis and characterization

The intermediate involved in PELD synthesis, PED, is also used in PEAD synthesis, as previously reported [17]. Briefly, PED is formed by the polycondensation of a 1:1 molar ratio of t-BOC aspartic acid and EGDE, followed by the removal of the BOC protecting group (Fig. 1a). t-BOC lysine is then conjugated and subsequently de-protected to form the final product. During the conjugation step, t-BOC lysine is activated by DCC and may then react intermolecularly as it contains an unprotected primary amine. PED is added immediately following activation to limit the amount of polylysine that forms before conjugation. This appears to have little effect on the functionality of the polycation for complexation with heparin; however, lysine with both amine groups protected may be used in the future for a more homogeneous product. Purification by repeated precipitations removes solvents and by-products until no impurity peaks are observed on the ^1H NMR spectrum. PELD was analyzed by ^1H NMR spectroscopy for chemical shifts distinctive of its structure (Fig. 1b). Protons in the ethylene glycol backbone produced shifts at $\delta 4.1$ and 4.4 and a multiplet between $\delta 3.4$ and 3.9 . Shifts between $\delta 1.2$ and 1.8 correspond to the aliphatic tail of lysine. FTIR analysis of PELD shows absorbance around 1665 cm^{-1} resulting from ester bonds and in the $3000\text{--}3500 \text{ cm}^{-1}$ range due to amide bonds and free hydroxyl groups (Fig. 1c). PELD had a T_g of $51.92 \text{ }^\circ\text{C}$, and no crystallization was observed between -50 and $+150 \text{ }^\circ\text{C}$ (Fig. 1d). GPC analysis indicated that PELD had a molecular weight (M_p) of approximately 3.5 kDa.

3.2. Characterization of PELD:heparin coacervates

When combined with polyanions such as heparin, PELD self-assembles into a coacervate. Coacervation is a liquid-liquid phase separation analogous to an emulsion except that the coacervate phase still contains water [23]. The PELD:heparin coacervate is visible as a turbid solution. The morphology of the PELD coacervate was observed by scanning electron microscopy (Fig. 1e) and reveals ribbon-like sheets and fibers, and globular structures. The

ribbon-like structures are on the micron scale and highly variable in size, while most globular beads are 1–5 μm .

A number of different PELD:heparin mass ratios ranging from 2.5 to 15 were further characterized. Zeta potential, a measure of the surface charge on a colloidal system, was analyzed first. As expected, a low PELD:heparin ratio yielded an overall negative surface charge, indicating an excess of anionic heparin (Fig. 2a). As the mass ratio increased, so did the zeta potential, reaching an overall neutral charge at a mass ratio of approximately 10. This indicates that heparin, the most negatively charged biomolecule, has approximately 10-fold greater charge density per unit mass compared to PELD. At mass ratios above 10, excess PELD molecules exist and create a positive surface charge. Zeta potential is also commonly used to estimate the stability of a colloidal system. Large positive or negative zeta potentials (generally +30 or –30 mV) indicate that the particles will tend to repel each other, while particles with low zeta potentials have little force to prevent aggregation.

The hydrodynamic diameter, or particle size, was also observed using DLS to assess how the PELD:heparin mass ratio and resultant surface charge affects the coacervate droplet size. The smallest droplet size was observed was 214 nm, at a mass ratio of 2.5, and the largest was 1208 nm, at a mass ratio of 7.5 (Fig. 2b). In general, large droplet sizes were observed around a mass ratio of 10, where the charge of the coacervate was near its isoelectric point. As the mass ratio was adjusted, and the zeta potential deviated from zero and the droplet size decreased. This is likely an effect of coacervate aggregation, further elucidated by polydispersity measurements.

The polydispersity index (PDI) in DLS measurements is calculated from the cumulant analysis of the DLS intensity autocorrelation function. It is arbitrarily scaled to a maximum value of 1. Values below 0.2 are typically considered monodisperse, while those greater than 0.7 are considered highly polydisperse. Coacervates bearing the highest surface charge (mass ratios of 2.5 and 15) were monodisperse (Fig. 2b). However, as the surface charge approaches neutrality, the repulsion force between coacervate droplets decreases and aggregations form more readily. We also expect the size of aggregations to vary, thereby increasing the PDI. Indeed, we observed that the PDI tended to increase as the coacervate surface charge approached neutrality, with a maximal PDI of 1 at a mass ratio of 10.

Mass ratios of 5 (negative), 10 (neutral) and 15 (positive) were selected for fluorescent imaging. Fluorescein, a small, charged dye, was added to the heparin solution and became incorporated into the coacervate upon addition of PELD. Droplets ranging from <1 μm to ~5 μm in diameter were observed in the negatively and positively charged coacervates, which appeared similar in size and distribution (Fig. 3). This correlates well with our DLS results, with the >1 μm droplets representing aggregates which led to the recorded polydispersity. The neutral coacervate had droplets ranging from 1 to 10 μm and was very polydisperse, as observed with DLS. Images were taken immediately after coacervation; therefore, aggregation probably occurs more quickly in neutral coacervates.

3.3. PELD cytocompatibility

Polycations typically carry high cytotoxicity, making them unsuitable in many translational applications [15]. Development of a biocompatible polycation which can deliver growth factors without affecting the cell response itself is of high importance. We tested the cytocompatibility of PELD using an established method for polycations with the fibroblast cell line, NIH 3T3 [24,25]. We compared PELD to PEI, a common polycation used in cell culture and as a polymer transfectant for non-viral gene delivery [26,27]. We also used PEAD as a positive control, as we have previously shown it to be highly biocompatible both in vitro and in vivo [17]. At concentrations up to 10 mg ml⁻¹ PELD had no effect on cell viability compared to PEAD (Fig. 4). Conversely, PEI induced a significant reduction in fibroblast viability at all concentrations, even as low as 0.01 mg ml⁻¹, compared to both PEAD and PELD. This toxicity of PEI has been well documented previously and exemplifies a major limitation of many polycations in scientific research [11]. These results indicate that PELD displays no in vitro cytotoxicity issues in a range of concentrations that are physiologically relevant, considering the dilution when applied in the body. Considering the biocompatibility of PEAD [17], it is unsurprising that utilizing the same design principle for lysine results in a lysine-based polycation that also has excellent biocompatibility.

3.4. Controlled release from PELD coacervates

The high cytocompatibility of PELD warranted further investigation of its suitability for controlled release of biomolecules. Heparin-binding sites often contain multiple cationic amino acids, rendering a high positive charge density which interacts with the many sulfate groups of heparin [28]. Therefore PELD competes with growth factors and other proteins for binding to heparin, and thus positively charged coacervates exhibit poor loading efficiency (data not shown). Only coacervates with negative zeta potential were investigated for release characteristics. We tested the loading and release of BSA from PELD:heparin coacervates of three different mass ratios over 21 days. BSA is commonly used as a model protein in drug delivery research and it also binds to heparin with a K_d of 4.3 μ M [29]. Observations common to all coacervates were high loading efficiencies of greater than 95%, low initial burst release and sustained release thereafter through to the end of the experiment (Fig. 5). A direct relationship between the charge and release rates was observed, with a more negative charge inducing a slower release of BSA from the coacervate. The total release after 21 days ranged from 17.4% to 58.8% for the -10 and 0 mV coacervates, respectively, with the -5 mV coacervate displaying an intermediate total release. We expect that multiple mechanisms play a role in the release of biomolecules: degradation of the polycation, as has been demonstrated with PEAD and similar polycations [17,30], dissociation of the coacervate in an ionic environment, and competition for heparin between the polycation and heparin-binding proteins. The dependence of release on charge supports the participation of the last mechanism. These data demonstrate that a high degree of control over release can be obtained by simply altering the PELD:heparin mass ratio of the coacervate.

3.5. Coacervate coating of polymeric scaffolds

The value of a controlled release vehicle for many tissue engineering approaches will hinge on its ability to coat a polymeric scaffold. The coacervate is highly charged and therefore

interacts by Coulombic forces with polymers bearing surface charge. It also contains many functional groups, such as hydroxyl groups on PEAD, which may form hydrogen bonds with polarized materials. Finally, the coacervate may participate in hydrophobic interactions with non-wetting surfaces as it is phase-separated from water.

We next tested the ability of the coacervate to adsorb to a porous PLGA disk as a model polymeric scaffold. When the turbid coacervate solution was exposed to the disk the optical density dropped rapidly (Fig. 6a). The change in optical density was directly proportional to the fraction of coacervate removed from the solution and adsorbed to the scaffold. The coacervate adsorbed rapidly and after 15 min reached a plateau at maximal fractional adsorption. Coacervate alone with no scaffold served as a control, and showed no significant change in optical density throughout the course of the experiment. After 30 min, coacervate-coated scaffolds were a yellow-orange color, similar to the color of PELD (Fig. 6b).

Coated and uncoated PLGA scaffolds were further analyzed by scanning electron microscopy (Fig. 7). The coacervate was clearly observable as a thin network which covered the surface of the PLGA material and also spanned a number of pores with spider's web-like morphology. However, the coating does not occlude the pores, allowing space for cells to infiltrate the scaffold. Coacervate is also clearly visible within the pores of the scaffold, indicating that it penetrated beyond the scaffold outer surface. This may be important for forming a chemokine gradient which extends into the scaffold for recruitment of cells. These data suggest that the coacervate delivery vehicle can be quickly and easily adsorbed onto polymeric tissue engineering scaffolds in aqueous solution to provide sustained release of heparin-binding growth factors or cytokines.

4. Conclusions

We designed a lysine-based polycation to interact polyvalently with intact heparin and spontaneously form a coacervate in aqueous solutions. Compared to the commonly used polycation PEI, PELD displayed significantly better cytocompatibility. Loading and release of BSA was tunable based on the PELD:heparin ratio of the coacervate. Finally, rapid adsorption of the coacervate onto polymeric scaffolds in water provides a simple means to integrate controlled release of biomolecules with tissue engineering scaffolds. These results suggest wide applicability of this polycation for controlled and sustained delivery of heparin-binding proteins.

Acknowledgments

The authors would like to thank Scientific Protein Laboratories LLC for their kind donation of the clinical-grade heparin, Dr. Zhengwei You for providing the PLGA scaffolds, Mr. Hongkun He for his help with GPC, and University of Pittsburgh's Center for Biological Imaging (CBI) for use of their scanning electron microscope. This work was supported by grants from the National Science Foundation (DMR 1005766), the American Heart Association (12EIA9020016) and the National Institutes of Health (2T32HL076124).

References

1. Godbey WT, Wu KK, Mikos AG. Poly(ethylenimine) and its role in gene delivery. *J Control Release*. 1999; 60:149–60. [PubMed: 10425321]

2. Agnihotri SA, Mallikarjuna NN, Aminabhavi TM. Recent advances on chitosan-based micro- and nanoparticles in drug delivery. *J Control Release*. 2004; 100:5–28. [PubMed: 15491807]
3. Ahn CH, Chae SY, Bae YH, Kim SW. Biodegradable poly(ethylenimine) for plasmid DNA delivery. *J Control Release*. 2002; 80:273–82. [PubMed: 11943404]
4. Borchard G. Chitosans for gene delivery. *Adv Drug Deliv Rev*. 2001; 52:145–50. [PubMed: 11718938]
5. Illum L, Jabbal-Gill I, Hinchcliffe M, Fisher AN, Davis SS. Chitosan as a novel nasal delivery system for vaccines. *Adv Drug Del Rev*. 2001; 51:81–96.
6. van der Lubben IM, Verhoef JC, Borchard G, Junginger HE. Chitosan and its derivatives in mucosal drug and vaccine delivery. *Eur J Pharm Sci*. 2001; 14:201–7. [PubMed: 11576824]
7. Illum L, Farraj NF, Davis SS. Chitosan as a novel nasal delivery system for peptide drugs. *Pharm Res*. 1994; 11:1186–9. [PubMed: 7971722]
8. Garcia-Fuentes M, Alonso MJ. Chitosan-based drug nanocarriers: where do we stand? *J Control Release*. 2012; 161:496–504. [PubMed: 22480607]
9. Kean T, Thanou M. Biodegradation, biodistribution and toxicity of chitosan. *Adv Drug Deliv Rev*. 2010; 62:3–11.
10. Lv H, Zhang S, Wang B, Cui S, Yan J. Toxicity of cationic lipids and cationic polymers in gene delivery. *J Control Release*. 2006; 114:100–9. [PubMed: 16831482]
11. Moghimi SM, Symonds P, Murray JC, Hunter AC, Debska G, Szewczyk A. A two-stage poly(ethylenimine)-mediated cytotoxicity: implications for gene transfer/therapy. *Mol Ther*. 2005; 11:990–5. [PubMed: 15922971]
12. De Smedt SC, Demeester J, Hennink WE. Cationic polymer based gene delivery systems. *Pharm Res*. 2000; 17:113–26. [PubMed: 10751024]
13. Choi YH, Liu F, Kim JS, Choi YK, Park JS, Kim SW. Polyethylene glycol-grafted poly-L-lysine as polymeric gene carrier. *J Control Release*. 1998; 54:39–48. [PubMed: 9741902]
14. Trubetsky VS, Torchilin VP, Kennel SJ, Huang L. Use of N-terminal modified poly(L-lysine)–antibody conjugate as a carrier for targeted gene delivery in mouse lung endothelial cells. *Bioconjug Chem*. 1992; 3:323–7. [PubMed: 1390987]
15. Fischer D, Li Y, Ahlemeyer B, Krieglstein J, Kissel T. In vitro cytotoxicity testing of polycations: influence of polymer structure on cell viability and hemolysis. *Biomaterials*. 2003; 24:1121–31. [PubMed: 12527253]
16. Hong S, Leroueil P, Janus E, Peters J, Kober M-M, Islam M, et al. Interaction of polycationic polymers with supported lipid bilayers and cells: nanoscale hole formation and enhanced membrane permeability. *Bioconjug Chem*. 2006; 17:728–34. [PubMed: 16704211]
17. Chu H, Gao J, Wang Y. Design, synthesis, and biocompatibility of an arginine-based polyester. *Biotechnol Prog*. 2012; 28:257–64. [PubMed: 22034156]
18. Chu H, Gao J, Chen CW, Huard J, Wang Y. Injectable fibroblast growth factor-2 coacervate for persistent angiogenesis. *Proc Natl Acad Sci USA*. 2011; 108:13444–9. [PubMed: 21808045]
19. Johnson NR, Wang Y. Controlled delivery of heparin-binding EGF-like growth factor yields fast and comprehensive wound healing. *J Control Release*. 2013; 166:124–9. [PubMed: 23154193]
20. Johnson NR, Wang Y. Controlled delivery of sonic hedgehog morphogen and its potential for cardiac repair. *PLoS One*. 2013; 8:e63075. [PubMed: 23690982]
21. Chu H, Chen CW, Huard J, Wang Y. The effect of a heparin-based coacervate of fibroblast growth factor-2 on scarring in the infarcted myocardium. *Biomaterials*. 2013; 34:1747–56. [PubMed: 23211448]
22. Gao J, Crapo PM, Wang Y. Macroporous elastomeric scaffolds with extensive micropores for soft tissue engineering. *Tissue Eng Part A*. 2006; 12:917–25.
23. De Kruijff CG, Weinbreck F, De Vries R. Complex coacervation of proteins and anionic polysaccharides. *Curr Opin Colloid Interface Sci*. 2004; 9:340–9.
24. Boussif O, Lezoualc'h F, Zanta MA, Mergny MD, Scherman D, Demeneix B, et al. A versatile vector for gene and oligonucleotide transfer into cells in culture and in vivo: polyethylenimine. *Proc Natl Acad Sci USA*. 1995; 92:7297–301. [PubMed: 7638184]

25. Moreau E, Domurado M, Chapon P, Vert M, Domurad D. Biocompatibility of polycations: in vitro agglutination and lysis of red blood cells and in vivo toxicity. *J Drug Target*. 2002; 10:161–73. [PubMed: 12074543]
26. Vancha AR, Govindaraju S, Parsa KV, Jasti M, Gonzalez-Garcia M, Ballesteros RP. Use of polyethyleneimine polymer in cell culture as attachment factor and lipofection enhancer. *BMC Biotechnol*. 2004; 4:23. [PubMed: 15485583]
27. Nguyen HK, Lemieux P, Vinogradov SV, Gebhart CL, Guerin N, Paradis G, et al. Evaluation of polyether–polyethyleneimine graft copolymers as gene transfer agents. *Gene Ther*. 2000; 7:126–38. [PubMed: 10673718]
28. Fromm JR, Hileman RE, Caldwell EE, Weiler JM, Linhardt RJ. Pattern and spacing of basic amino acids in heparin binding sites. *Arch Biochem Biophys*. 1997; 343:92–100. [PubMed: 9210650]
29. Lee MK, Lander AD. Analysis of affinity and structural selectivity in the binding of proteins to glycosaminoglycans: development of a sensitive electrophoretic approach. *Proc Natl Acad Sci USA*. 1991; 88:2768–72. [PubMed: 1901416]
30. Zern BJ, Chu HH, Osunkoya AO, Gao J, Wang YD. A biocompatible arginine-based polycation. *Adv Funct Mater*. 2011; 21:434–40. [PubMed: 23393493]

Appendix A. Figures with essential colour discrimination

Certain figures in this article, particularly Figs. 3 and 6, are difficult to interpret in black and white. The full colour images can be found in the on-line version, at <http://dx.doi.org/10.1016/j.actbio.2013.09.012>

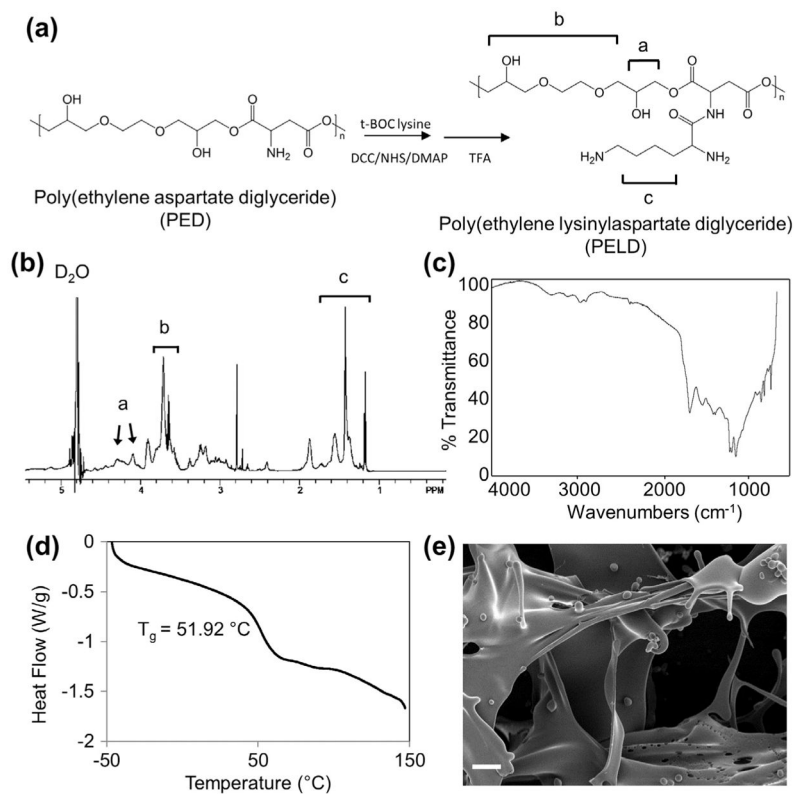


Fig. 1. Synthesis and characterization of PELD and PELD:heparin coacervate. (a) The intermediate PED, synthesized by polycondensation of EGDE and aspartic acid. PELD was formed by the conjugation of t-BOC lysine to aspartic acid in PED. Groups producing characteristic chemical shifts in the ^1H NMR spectrum are indicated. (b) The ^1H NMR spectrum of PELD showing signals characteristic of lysine and a backbone composed of glycerol and aspartic acid. D_2O is observed at $\delta 4.8$. (c) FTIR spectrum of PELD showing ester stretches at 1665 cm^{-1} and weak amide and hydroxyl stretches near 3000 cm^{-1} . (d) DSC thermogram indicates a glass transition temperature of $51.92\text{ }^{\circ}\text{C}$. (e) Scanning electron micrograph of lyophilized PELD:heparin coacervate displaying both ribbon-like sheets and globular domains. Scale bar = $10\text{ }\mu\text{m}$.

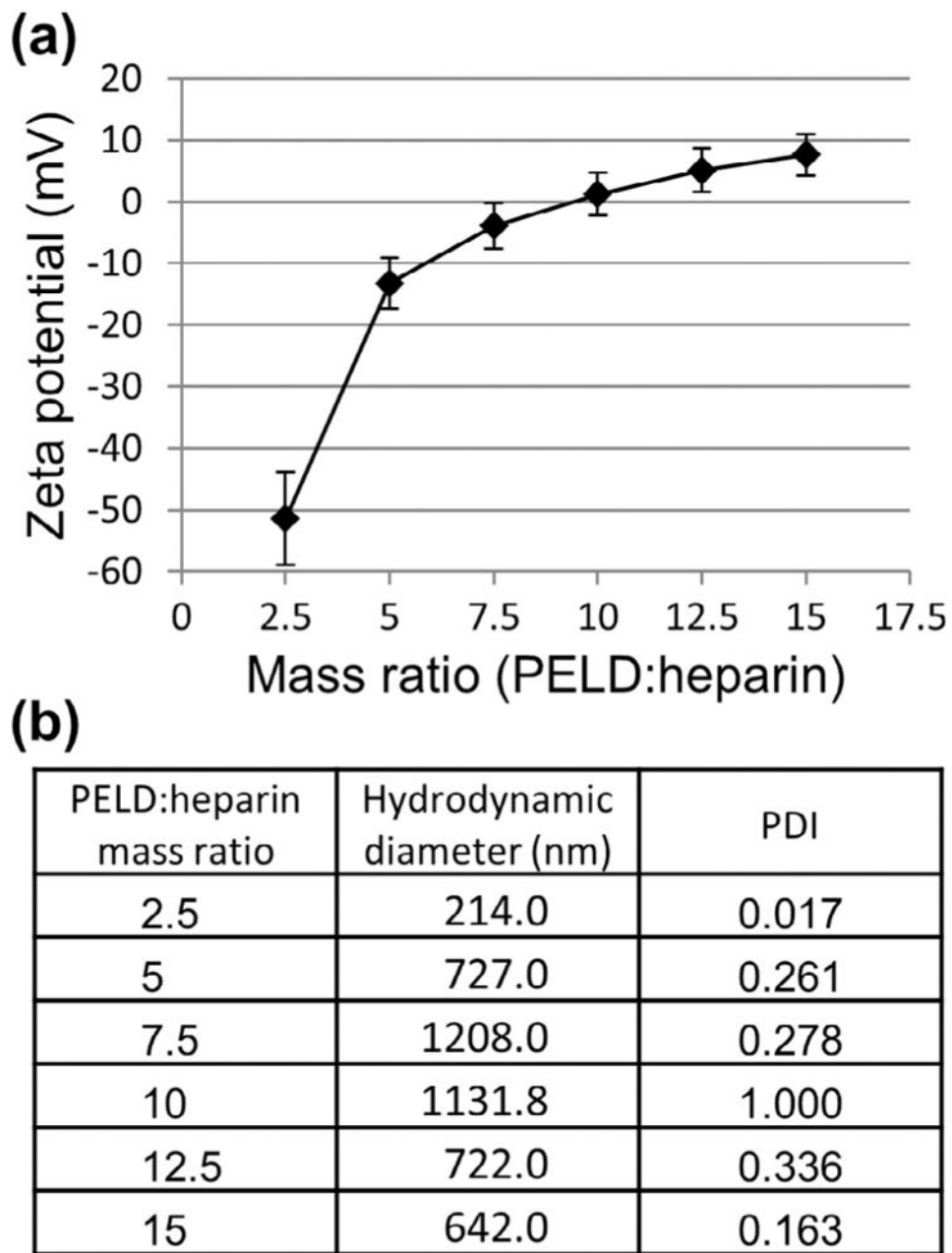


Fig. 2. Zeta potential and hydrodynamic diameter of PELD:heparin coacervates. PELD was combined with heparin at different mass ratios to form coacervates. (a) Zeta potential measurements reveal surface charge of coacervates, with an isoelectric point (charge neutrality) at a mass ratio of 10. (b) DLS measurements of the hydrodynamic diameter and polydispersity of the coacervates. The hydrodynamic diameter represents the average size of the coacervate droplets in water. The PDI is arbitrarily limited to a maximum value of 1, with values < 0.2 being considered monodisperse and values > 0.7 indicating high polydispersity.

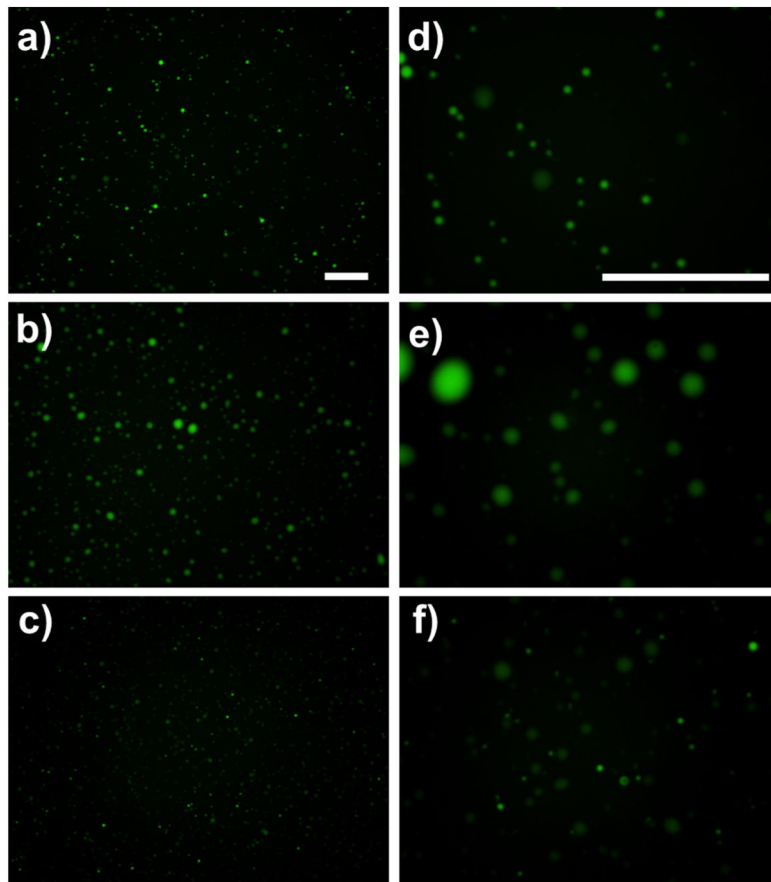


Fig. 3. Fluorescent imaging of coacervates. Fluorescein, a charged fluorescent dye, was incorporated into the coacervate to enable imaging by fluorescent microscopy. $\times 10$ Magnification images of coacervates with PELD:heparin mass ratios of (a) 5, (b) 10 and (c) 15. (d–f) High-magnification ($\times 40$) images of a–c, respectively. Scale bars = 100 μm .

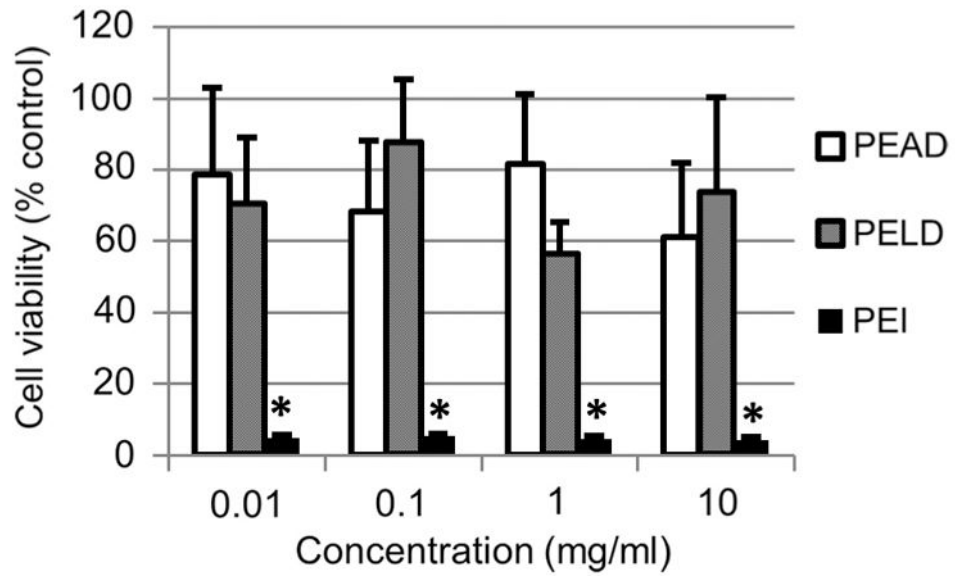


Fig. 4. Polycation cytotoxicity. NIH3T3 fibroblasts were exposed to PEAD, PELD or PEI dissolved in culture medium at 0.01, 0.1, 1 or 10 mg ml⁻¹. Cell viability was measured after 24 h by Live/Dead Assay. * $p < 0.01$ compared to both PEAD and PELD groups.

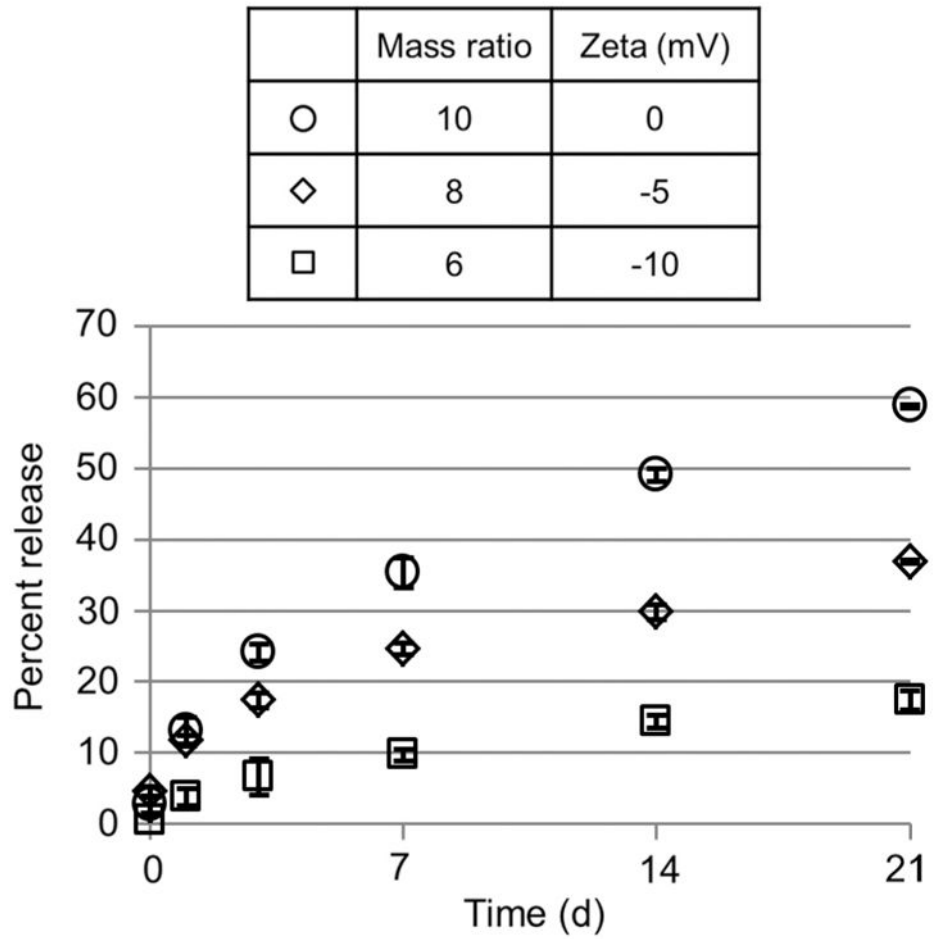


Fig. 5. BSA release from coacervates. PELD:heparin mass ratios of 10, 8 and 6 were used, which correspond to zeta potentials of approximately 0, -5 and -10 mV, respectively. Each coacervate was loaded with 500 μ g BSA, and release was quantified on days 0, 1, 3, 7, 14 and 21 by total protein assay.

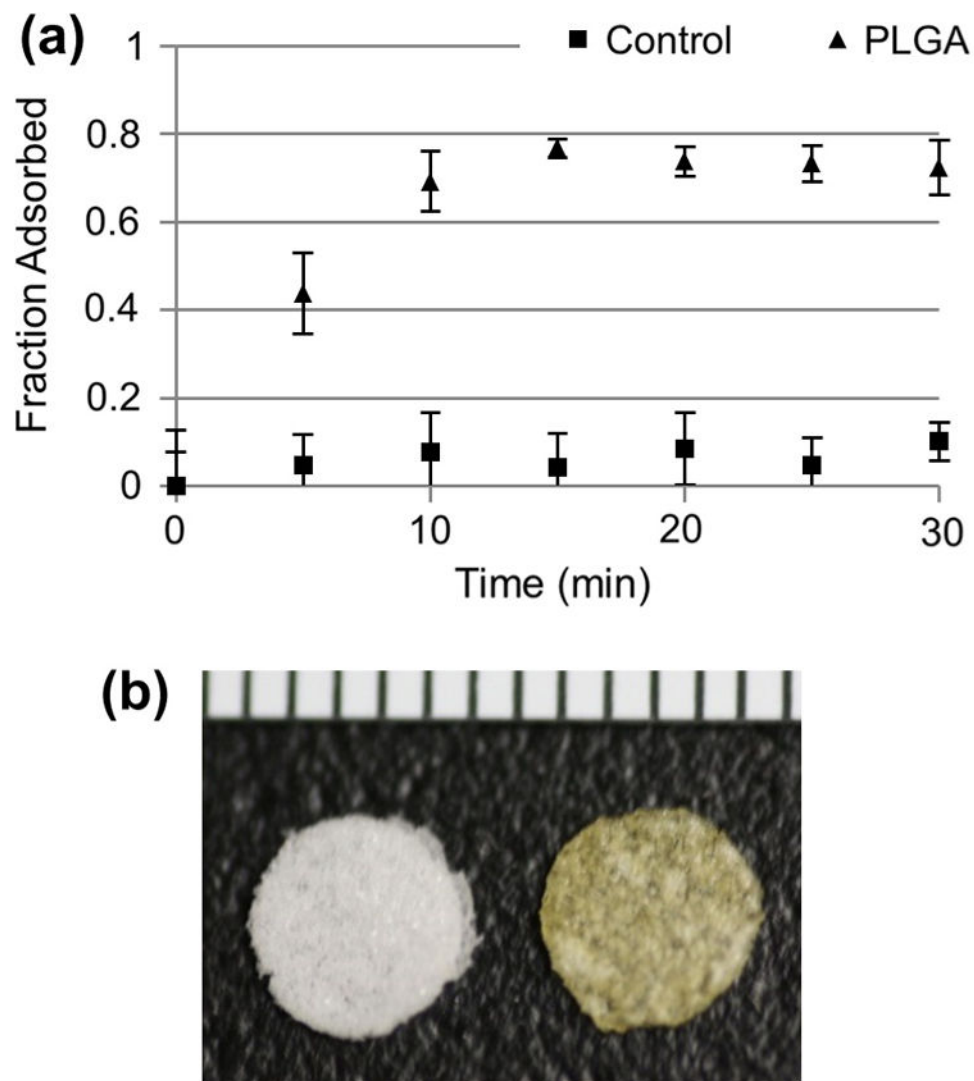


Fig. 6. Adsorption of PELD coacervate to polymer scaffolds. PELD coacervate was prepared in water and then porous PLGA scaffolds were added. (a) Coacervate adsorption to the scaffold was measured as a fractional change in optical density. A control coacervate solution did not receive a scaffold. (b) PELD coacervate-coated scaffold (right) next to a bare PLGA scaffold (left) at the endpoint of the experiment. Ruler units are 1 mm.

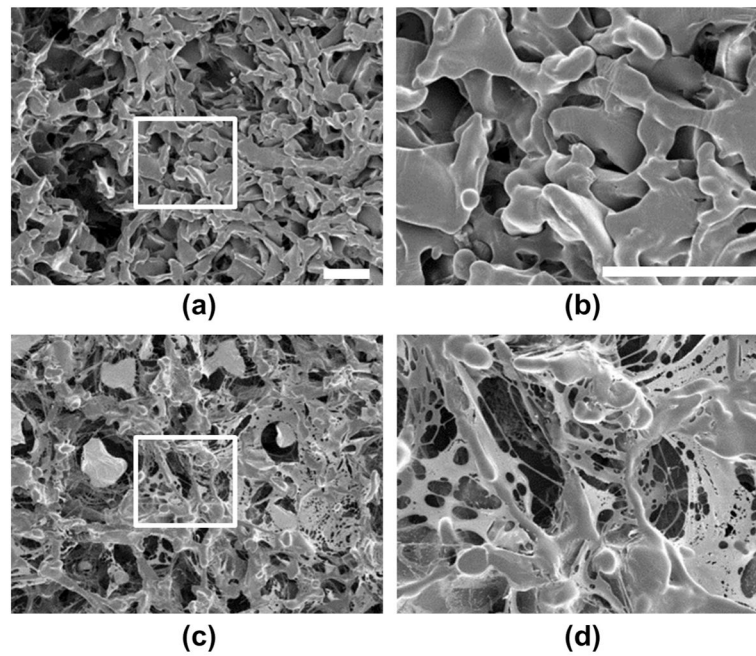


Fig. 7. Scanning electron micrographs of PELD coacervate adsorbed to scaffolds. PLGA scaffolds with a 75–150 μm pore size were prepared by the salt-leaching method and imaged by SEM. (a) Uncoated PLGA scaffold ($\times 150$ magnification). (b) Coated PLGA scaffold, submerged in PELD coacervate solution in water for 5 min, then lyophilized and imaged ($\times 150$ magnification). (c, d) High-magnification ($\times 500$) SEM images of the indicated areas of (a) and (b), respectively. All scale bars = 100 μm .